

Structural Basis for Ligand Exchange on Au₂₅(SR)₁₈

Thomas W. Ni, Marcus A. Tofanelli, Billy D. Phillips, and Christopher J. Ackerson*

Department of Chemistry, Colorado State University, Fort Collins, Colorado 80525, United States

Supporting Information

ABSTRACT: The single-crystal X-ray structure of Au₂₅(SC₂H₄Ph)₁₆(pBBT)₂ is presented. The crystallized compound resulted from ligand exchange of Au₂₅(SC₂H₄Ph)₁₈ with pBBT as the incoming ligand, and for the first time, ligand exchange is structurally resolved on the widely studied Au₂₅(SR)₁₈ compound. A single ligand in the asymmetric unit is observed to exchange, corresponding to two ligands in the molecule because of the crystallographic symmetry. The ligand-exchanged Au₂₅ is bonded to the most solvent-exposed Au atom in the structure, making the exchange event consistent with an associative mechanism. The apparent nonexchange of other ligands is rationalized through possible selective crystallization of the observed product and differential bond lengths.

Ligand-exchange reactions on metal nanoparticles^{1–3} are widely used to integrate nanoparticles into devices or enable applications.^{4,5} Such reactions are also of fundamental interest because mixed-ligand shells arising after ligand exchange exert a profound influence on the optical,⁶ electronic,⁷ and assembly properties⁸ of gold nanoparticles.

The Au₂₅(SR)₁₈ cluster is a widely studied and accessible model system for understanding the broad class of thiolate-protected gold nanoparticles and clusters.⁹ The compound is isolable in 1–/0/1+ charge states,¹⁰ and the X-ray structures of the anion^{11,12} and neutral^{13,14} compounds are solved. Most Au₂₅(SR)₁₈ clusters crystallize in *P*T̄, meaning that there is only *i* symmetry. The crystal structures universally show an icosahedral core of 13 atoms, with the remaining 12 Au atoms held in “semirings” of SR–Au^I–SR–Au^I–SR construction. Herein we refer to the central SR ligand in the semiring as the apex ligand and the terminal ligands as core ligands (Figure S1 in the Supporting Information, SI).

Previous studies on the relative chemical reactivity of core and apex ligands are ambiguous. One study shows that apex ligands are more prone to oxidation and suggested as thus being less stable.¹⁵ However, bond lengths are shorter for Au^I–SR than for Au(core)–SR, suggesting that core ligands may be less stable. It is unclear which type of ligand may be more reactive in a ligand-exchange reaction.

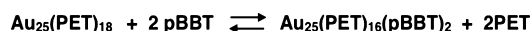
Previous work on ligand exchange for all thiolate-protected gold clusters generally suggests an associative mechanism^{1,2,16,17} and was mostly completed prior to structural knowledge of the cluster. Interpretations of this kinetic data assumed a structural model in which ligands bond to clear edge, vertex, and face sites. Because the structural nature of the gold–sulfur interface¹⁸ does

not include such sites, it is unclear how to explain the multiple kinetic environments.

Recently, it was shown that each of the 18 possible ligand-exchange products can be isolated by column chromatography.¹⁹ Despite the intensive study of this compound for structural, chemical, and catalytic purposes, there are no prior structures of ligand-exchanged Au₂₅ to our knowledge.

Here we present the first crystal structure of partially exchanged Au₂₅(SR)₁₈. The ligand-exchange reaction was done on a short time scale, isolating ligand sites corresponding to previously identified kinetic “fast exchange”. In our crystal structure, we observe the exchange of 1 of the 9 symmetry unique ligands (Figure S2 in the SI), in a position that is consistent with an associative mechanism.

Ligand exchange was accomplished by the reaction shown in Scheme 1. Briefly, Au₂₅(SC₂H₄Ph)₁₈⁰, hereafter Au₂₅(PET)₁₈,

Scheme 1. Ligand Exchange of Au₂₅(PET)₁₈ with pBBT

was exposed to a 5-fold molar excess of *p*-bromobenzenethiol (pBBT) for 7 min in CH₂Cl₂, resulting in products corresponding to the fast ligand-exchange environment for this cluster. A full description of the experimental details is in the SI. Single crystals of the crude product were grown by slow cooling from a saturated toluene/ethanol solution.

Diffraction patterns were recorded at the Advanced Light Source (ALS) as described in the methods. The diffraction patterns were indexed to *P*T̄ in XDS²² and XPREP (version 6.12; Bruker AXS: Madison, WI, 1999). Refinement of the structure of the ligand-exchanged Au₂₅ was done in SHELX.²⁰

Static substitutional refinement in SHELX was used to determine the occupancy of both original (PET) and incoming (pBBT) ligands in each of the nine symmetry-unique ligand positions. We number each symmetry-unique ligand from 1 to 9 according to the observed or expected reactivity for ligand exchange (vide infra), and we numbered each Au atom according to the same convention. In the coordinate file, the numbering of each S headgroup identifies the ligand number.

The occupancy by the pBBT ligand was refined to 74.6% for ligand 1. Static substitutional refinement in each of the other eight ligand positions either failed to refine or refined to zero pBBT occupancy. Figure 1 shows a rendering of the crystal structure, highlighting the exchanged ligand.

The exchange of this unique ligand site can be explained by a combination of the solvent accessibility of Au atoms bonded to

Received: May 12, 2014

Published: June 23, 2014

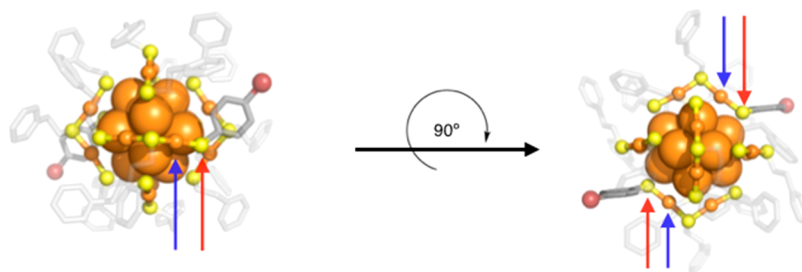


Figure 1. Single-crystal X-ray structure of $\text{Au}_{25}(\text{PET})_{16}(\text{pBBT})_2$. Color code: orange, Au; yellow, S; gray, C; red, Br. Red arrows point to the S headgroup of ligand 1 and blue arrows to Au1.

the ligands and noncovalent interactions of ligands within the ligand shell. Solvent exposure of Au atoms bonded to S ligand headgroups is a requisite for the expected associative ligand exchange because the solvent-exposed area represents a surface capable of bonding to an incoming ligand.²¹ Noncovalent ligand interactions in the ligand shell may stabilize certain ligands against exchange, even if they are bonded to solvent-exposed Au atoms.

The solvent-accessible surface area was calculated with *PyMOL*²³ (Schrödinger, LLC). A total of 3 of the 13 Au atoms in the asymmetric unit have some degree of solvent exposure. Each of these Au atoms is in a semiring; each of the six semirings of the Au_{25} cluster contains one solvent-exposed Au^I atom. According to our numbering convention, the solvent-exposed Au^I atoms in the asymmetric unit are Au1, Au2, and Au3 (Figure 2). The calculated solvent exposure (assuming a solvent probe

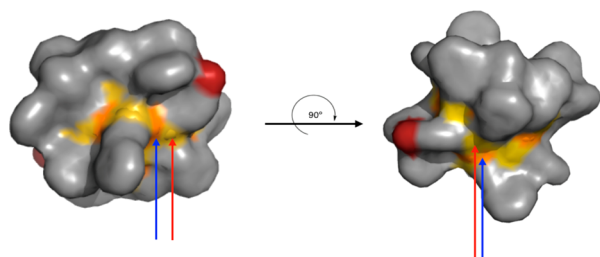


Figure 2. Solvent-exposed surface area of $\text{Au}_{25}(\text{PET})_{16}(\text{pBBT})_2$. The orientation of the molecules and color schemes are identical with those in Figure 1. The probe radius used is 1.76 nm. Red arrows point to the S headgroup of ligand 1 and blue arrows to Au1.

radius of 1.76 Å corresponding to CH_2Cl_2 to approximate the effective size of the CH_2Cl_2 molecule) of Au1 is 3.53 \AA^2 , followed by Au2 and Au3 with 1.8 \AA^2 and 1.94 \AA^2 , respectively. In the present crystal structure, ligand exchange occurs only for the ligand bonded to Au1, the most solvent-exposed Au atom. This is structurally consistent with an associative mechanism. It is also consistent with our results for structural ligand exchange on $\text{Au}_{102}(\text{SR})_{44}$.²¹

There are five other ligands attached to solvent-accessible Au atoms in the asymmetric unit: ligands 2–6. Ligand 4 is the apex ligand of Au1. Ligands 2 and 5 are core and apex ligands of Au2. Ligands 3 and 6 are core and apex ligands of Au3.

Ligand 4, like ligand 1, is bonded to Au1. We rationalize the nonexchange of the apex-positioned ligand 4, in part, by comparing the bond lengths as a proxy for bond strength. Ligand 4 Au–SR–Au bond lengths are 2.284 and 2.309 Å, while ligand 1 bond lengths are 2.280 and 2.390 Å. These bond lengths suggest that the ligand we observed to exchange is more weakly bonded.

The nonexchange of ligands 2–6, despite their bonding to solvent-accessible Au atoms, is puzzling, especially in the cases of ligands 2 and 3. That nearly 80% of ligand 1 is exchanged and there is no evidence of exchange of ligands 2 or 3 is inconsistent with the typical observation of ligand exchange, resulting in a distribution of products.¹⁹

To rationalize the exchange of only 1 of the 9 symmetry unique ligands, we analyzed the crystal contacts of the ligands in *Mercury*²⁴ (CCDC). This analysis reveals the interactions summarized in Table 1 and discussed in greater detail in the

Table 1. List of Inter- and Intramolecular Interactions Observed in the Crystal Structure

Au atom	ligand	contacts	
		intramolecular	intermolecular
1	1 (core)	ligand 3	ligand 8 (substantial)
1	4 (apex)		toluene
2	2 (core)		ligand 2
2	5 (apex)		
3	6 (apex)		ligand 9–phenyl–phenyl
3	3 (core)	ligand 1	

SI. We do note, however, that the exchange of pBBT into ligand position 1 generates several favorable crystal contacts, possibly reinforced by π interactions, compared to the native PET ligand. This substantial set of contacts is shown in Figure S3 in the SI. Thus, it is possible that the ligand exchange that we solved crystallographically results from selective crystallization of one of several products of the ligand-exchange reaction.

In conclusion, we present the first structure of $\text{Au}_{25}(\text{SR})_{18}$ after ligand exchange. We observe ligand exchange for ligands bonded to only the most solvent-accessible Au atoms in the structure. Crystal contact analysis suggests that we may have crystallized a subset of the possible ligand-exchange products. The exchange occurring only for ligands bonded to solvent-exposed Au atoms is consistent with previous kinetic and structural studies of ligand exchange on $\text{Au}_n(\text{SR})_m$ nanoclusters.

■ ASSOCIATED CONTENT

📄 Supporting Information

X-ray crystallographic data in CIF format, experimental details, data collection, structures, and coordinates of the crystal structure. This material is available free of charge via the Internet at <http://pubs.acs.org>.

■ AUTHOR INFORMATION

Corresponding Author

*E-mail: ackerson@colostate.edu.

Notes

The authors declare no competing financial interest.

■ ACKNOWLEDGMENTS

We thank the Colorado State University and the American Federation for Aging Research for funding this work. We thank Hannu Hakkinen and Kirsi Salorinne for useful discussions. The ALS is supported by the Director, Office of Science, Office of Basic Energy Sciences, of the U.S. Department of Energy under Contract DE-AC02-05CH11231.

■ REFERENCES

- (1) Hostetler, M.; Templeton, A.; Murray, R. *Langmuir* **1999**, *15*, 3782–3789.
- (2) Song, Y.; Murray, R. *J. Am. Chem. Soc.* **2002**, *124*, 7096–7102.
- (3) Templeton, A.; Cliffl, D.; Murray, R. *J. Am. Chem. Soc.* **1999**, *121*, 7081–7089.
- (4) Ackerson, C. J.; Powell, R. D.; Hainfeld, J. F. *Methods Enzymol.* **2010**, *481*, 195–230.
- (5) Sousa, A. A.; Morgan, J. T.; Brown, P. H.; Adams, A.; Mudiyansele, P.; Zhang, G.; Ackerson, C. J.; Kruhlak, M. J.; Leapman, R. D. *Small* **2012**, *8*, 2277–2286.
- (6) Mulvaney, P. *Langmuir* **1996**, *12*, 788–800.
- (7) Hicks, J.; Templeton, A.; Chen, S.; Sheran, K.; Jasti, R.; Murray, R.; Debord, J.; Schaaff, T.; Whetten, R. *Anal. Chem.* **1999**, *71*, 3703–3711.
- (8) Mirkin, C.; Letsinger, R.; Mucic, R.; Storhoff, J. *Nature* **1996**, *382*, 607–9.
- (9) Parker, J. F.; Fields-Zinna, C. A.; Murray, R. W. *Acc. Chem. Res.* **2010**, *43*, 1289–1296.
- (10) Tofanelli, M. A.; Ackerson, C. J. *J. Am. Chem. Soc.* **2012**, *134*, 16937–16940.
- (11) Heaven, M. W.; Dass, A.; White, P. S.; Holt, K. M.; Murray, R. W. *J. Am. Chem. Soc.* **2008**, *130*, 3754–3755.
- (12) Zhu, M.; Aikens, C. M.; Hollander, F. J.; Schatz, G. C.; Jin, R. *J. Am. Chem. Soc.* **2008**, *130*, 5883–5885.
- (13) Zhu, M.; Eckenhoff, W. T.; Pintauer, T.; Jin, R. *J. Phys. Chem. C* **2008**, *112*, 14221–14224.
- (14) Dainese, T.; Antonello, S.; Gascón, J. A.; Pan, F.; Perera, N. V.; Ruzzi, M.; Venzo, A.; Zoleo, A.; Rissanen, K.; Maran, F. *ACS Nano* **2014**, *8*, 3904–3912.
- (15) Wu, Z.; Jin, R. *ACS Nano* **2009**, *3*, 2036–2042.
- (16) Kassam, A.; Bremner, G.; Clark, B.; Ulibarri, G.; Lennox, R. *J. Am. Chem. Soc.* **2006**, *128*, 3476–3477.
- (17) Wong, O. A.; Heinecke, C. L.; Simone, A. R.; Whetten, R. L.; Ackerson, C. J. *Nanoscale* **2012**, *4*, 4099–4102.
- (18) Häkkinen, H. *Nat. Chem.* **2012**, *4*, 443–455.
- (19) Niihori, Y.; Matsuzaki, M.; Pradeep, T.; Negishi, Y. *J. Am. Chem. Soc.* **2013**, *135*, 4946–4949.
- (20) Sheldrick, G. M. *Acta Crystallogr., Part A* **2008**, *64*, 112–122.
- (21) Heinecke, C. L.; Ni, T. W.; Malola, S.; Makinen, V.; Wong, O. A.; Häkkinen, H.; Ackerson, C. J. *J. Am. Chem. Soc.* **2012**, *134*, 13316–13322.
- (22) Kabsch, W. *Acta Crystallogr., Part D* **2010**, *66*, 125–132.
- (23) *The PyMOL Molecular Graphics System*, version 1.5.0.4; Schrödinger, LLC: Portland, OR, 2014.
- (24) McCrae, C. F.; Edgington, P. R.; McCabe, P.; Pidcock, E.; Shields, G. P.; Taylor, R.; Towler, M.; van De Streek, J. *J. Appl. Crystallogr.* **2006**, *39*, 453–457.